



# **Universidad de Monterrey**

**Facultad de Ingeniería y Tecnología  
Ingeniería en Sistemas Computacionales**

## **Automatic classification of plutonic rocks with machine learning applied to extracted colors on iOS devices**

**Sarah Hernández Serrano  
1170469**

**Asesor: Dr. Germán Harvey Alférez Salinas  
Asesores secundarios: Dr. Benjamin Clausen y Dra. Ana María Martínez Ardila**

**Monterrey, Nuevo León, México  
00 de mayo de 2021**

### Abstract

The classification of different rocks can provide important information about the conditions under they were formed and their tectonic environment. Color is a key property for rock classification. However, it is difficult to describe the colors in rocks because the perceived colors depend on the observer's experience. Moreover, the equipment for rock classification is expensive, which makes this equipment prohibitive to geology students and amateurs. The contribution of this research work is fourfold. First, since color is a key property for rock classification, feature reduction was applied to several patches of plutonic rock images extracting just their four dominant colors by means of the k-means clustering method. Second, different machine learning models were created and evaluated by means of applying the Logistic Regression (LR), K-Nearest Neighbors (KNN), Decision Trees (DT), Support Vector Machine (SVM), and a Convolutional Neural Network (CNN) algorithms to a dataset with the extracted dominant colors. The best results were achieved with the KNN model: 93% of accuracy, 93% of precision, 93% of recall, and 93% of F1-score. Third, we present an iOS application that uses the KNN model to classify images of the following plutonic rocks: granite, granodiorite, gabbro, and diorite. The accuracy results of the iOS mobile application in the field were: 85.7% for granite, 20% for granodiorite, 70% for gabbro, and 28.5% for diorite. Fourth, we compared the results in the field with our previous work in which a CNN was trained using all the images features of the same dataset of plutonic rocks and deployed in an Android application.

### Index Terms

Machine Learning, Color Extraction, iOS Devices, Geology, Rock Classification, Features Reduction, Dominant Colors, K-means Clustering, Logistic Regression, K-Nearest Neighbors, Support Vector Machine, Convolutional Neural Network, Decision Trees.

## CONTENTS

<b>I</b>	<b>Introduction</b>	<b>1</b>
I-A	Background . . . . .	1
I-B	Problem Statement . . . . .	1
I-C	Justification . . . . .	1
I-D	Objectives . . . . .	1
I-E	Hypothesis . . . . .	2
<b>II</b>	<b>Theoretical Foundation</b>	<b>2</b>
II-A	Underpinnings of our Approach . . . . .	2
II-A1	Plutonic rocks . . . . .	2
II-A2	Machine Learning . . . . .	2
II-A3	Dominant colors . . . . .	3
II-A4	Underlying technologies . . . . .	3
II-B	Related Work . . . . .	3
II-B1	Image classification of rock lithology using machine learning . . . . .	4
II-B2	Rock classification with machine learning on Android devices . . . . .	5
II-B3	Recognition of mineral images applying machine learning and feature extraction . . . . .	5
II-B4	Discussion . . . . .	5
<b>III</b>	<b>Results</b>	<b>6</b>
III-A	Methodology . . . . .	6
III-A1	Getting the images of the plutonic rocks . . . . .	6
III-A2	Preparing the data . . . . .	6
III-A3	Determining the best number of color clusters . . . . .	6
III-A4	Color extraction . . . . .	6
III-A5	Data normalization and label encoding . . . . .	7
III-A6	Training the different algorithms with the extracted dominant colors . . . . .	7
III-A7	Evaluation of the machine learning algorithms . . . . .	8
III-B	Results . . . . .	9
III-C	Discussion . . . . .	11
<b>IV</b>	<b>Conclusions and Future Work</b>	<b>11</b>

# Automatic classification of plutonic rocks with machine learning applied to extracted colors on iOS devices

Sarah Hernández, Germán H. Alférez, Benjamin Clausen and Ana M. Martínez

*School of Engineering and Technology, Montemorelos University, Mexico*

## I. INTRODUCTION

### A. Background

The classification of different rocks can provide important information about the conditions under which they were formed. They can also tell us much about their tectonic environment, given that they are closely linked to the convection of tectonic plates. Also, their mineral and chemical makeup can be used to learn about the composition, temperature and pressure that exists within the Earth's mantle.

Plutonic rocks are a type of igneous rocks (one of the three main types of rocks in the world and also the most common) formed when magma in the middle of the volcanoes cools and solidifies below the Earth's surface. They come in many different sizes and colors, and have a wide variety of uses [1, 2].

Our contribution is fourfold. First we extracted the dominant colors of plutonic rock images grouping the image pixels according to their color in the RGB (Red, Green, Blue) and CIELab ( $L^*a^*b^*$ ) color spaces with the k-means algorithm. Color changes in rocks may indicate changes in the rock's mineral assemblage, texture, organic carbon content (shales), or other properties [3]. That is why color is a key property for rock classification. Second, we used the data of the dominant colors to create and evaluate several machine learning models with the following algorithms: Logistic Regression (LR), K-Nearest Neighbors (KNN), Decision Trees (DT), Support Vector Machine (SVM), and a Convolutional Neural Network (CNN). Third, we deployed the best model in an iOS application that classifies extracted colors in images into four types of plutonic rocks obtaining the following accuracy results in the field: 85.7% for granite, 20% for granodiorite, 70% for gabbro, and 28.5% for diorite. Fourth, we compared our approach with our previous work [ref] in which a CNN was trained with the same dataset of plutonic rock using the

whole set of image pixel features instead of the four dominant colors.

### B. Problem Statement

The equipment for rock classification is expensive, which makes it prohibitive to geology students and amateurs. In addition, there is a lack of mobile tools for plutonic rock classification with machine learning. Despite the fact that color is a key property for rock classification, it is an attribute difficult to describe because perceived colors in rocks also depend on the observer's experience with similar observations; so a color may often be named differently by different persons [3].

### C. Justification

There are two reasons to create an iOS mobile application that allows the classification of plutonic rocks with machine learning using their dominant colors. The dominant colors represent the principal color values of all the pixels in an image. First, no such application exists. A mobile application offers the flexibility to carry out the classification on real time and could be an alternative to expensive traditional methods of rock classification. Second, in our previous work we found that the accuracy of the model decreased in the field. We extracted the dominant colors to verify if feature reduction leads to better results in the field than the obtained with the Android application [ref] of our previous work using all the rock image features.

### D. Objectives

The main objective of this research work is to extract dominant colors from plutonic rock images to train several machine learning algorithms and deploy the best model in an iOS app. The results in the field are compared with our previous work [ref]. This objective is achieved with the following sub-objectives:

- Determine the best  $k$  number of clusters to use in the k-means clustering machine learning method to extract the dominant colors in terms of RGB and CIELab color spaces from images of plutonic rocks.
- Use the extracted dominant colors and the percentage of pixels belonging to each color cluster as the input to train

Sarah Hernández is a computer science engineering student at the School of Engineering and Technology of Montemorelos University, Nuevo León, Mexico, e-mail: 1170469@alumno.um.edu.mx.

Germán H. Alférez, Ph.D., is the director of the Institute of Data Science and professor at the School of Engineering and Technology of Montemorelos University, Nuevo León, Mexico, e-mail: harveyalferez@um.edu.mx.

Benjamin Clausen, Ph.D., is a professor at the Department of Earth and Biological Sciences of Loma Linda University, California, USA, e-mail: bclausen@llu.edu.

Ana M. Martínez, Ph.D., is a professor at the Department of Earth and Biological Sciences of Loma Linda University, California, USA, e-mail: anmartinez@llu.edu.

the following machine learning algorithms: LR, KNN, DT, SVM, and a CNN.

- Validate the models generated to get the best suited model and deploy it in an iOS mobile application.
- Test the effectiveness of the application with images taken from new plutonic rocks in the field. The results are compared with our previous work in which a CNN was trained with images using the whole set of features.

### E. Hypothesis

The training of a machine learning model with just the dominant colors extracted from granite, granodiorite, gabbro, and diorite images can provide an effective way for the classification of these plutonic rocks.

## II. THEORETICAL FOUNDATION

### A. Underpinnings of our Approach

Our approach is based on the following concepts (see Fig. 1).

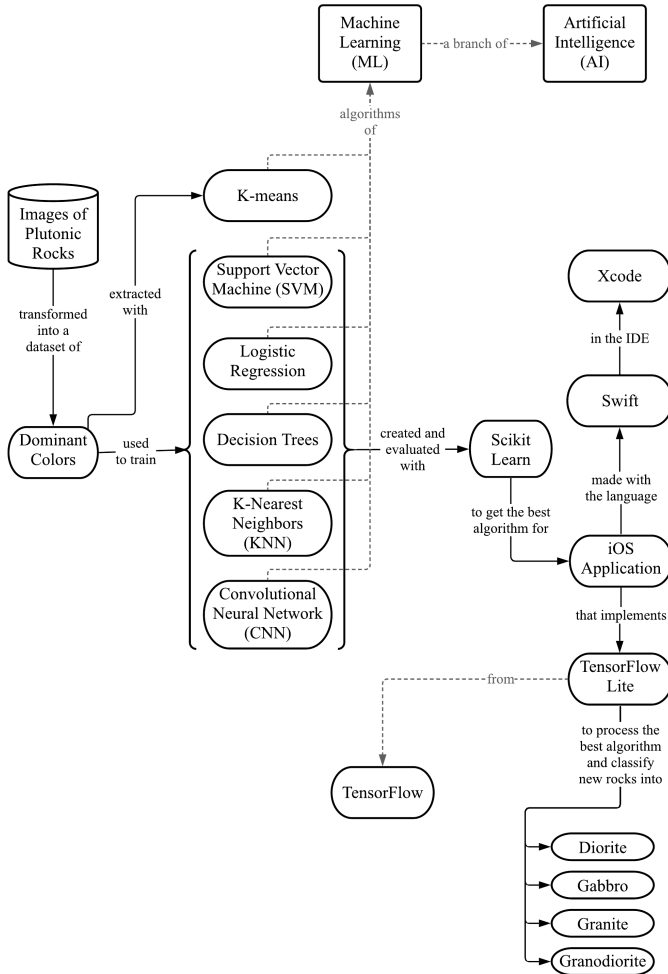


Figure 1. Underpinnings of our approach

### 1) Plutonic rocks

Plutonic rocks are solidified inside the Earth's crust, usually from magma, although they may have been formed by a different mechanism. Plutonic rocks are generally coarse-grained, but not all coarse-grained rocks are plutonic. According to [4]:

- Granite rocks are plutonic rocks with a granular texture, composed of similar amounts of quartz, potassium feldspar, and plagioclase as essential minerals, and smaller amounts of one or more minerals, such as biotite, muscovite or hornblende.
- Granodiorite is a plutonic rock of the granitoid family, characterized by quartz because plagioclase constitutes more than 2/3 of the total feldspars. Generally, together with granite, it is the most abundant rock of the great batholiths. Its volcanic equivalent is dacite. Granodiorite is similar to granite, but with less potassium feldspar and more plagioclase.
- Gabbro is a plutonic rock composed mainly of calcium plagioclase and clinopyroxene or orthopyroxene, with or without olivine or amphibole. It is the intrusive equivalent of basalt. It is distinguished from diorite by the nature of plagioclase, which is higher in calcium than in sodium.
- Diorite has about the same structural properties as granite but darker color and more limited supply. Commonly is composed of about two-thirds plagioclase feldspar and one-third dark-coloured minerals, such as hornblende or biotite. The presence of sodium-rich feldspar, oligoclase or andesine, in contrast to calcium-rich plagioclase, labradorite or bytownite, is the main distinction between diorite and gabbro [5].

### 2) Machine Learning

Machine learning is a branch of artificial intelligence that lies at the intersection of computer science, engineering and statistics, and often appears in other disciplines. Machine learning systems can be classified according to the type of supervision they get during training [6, 7]. In this way, there are two major categories:

#### a) Supervised learning

In supervised learning, the training set fed to the algorithm includes the desired solutions, called labels. A typical supervised learning task is classification [7]. Some common algorithms of supervised learning are described as follows:

- Logistic Regression (LR) is commonly used to estimate the probability of an instance to belong to a particular class. This model computes a weighted sum of the input features (plus a bias term) and outputs the logistic of this result. The logistic is a sigmoid function that outputs a number between 0 and 1. This makes it a binary classifier [7].
- K-Nearest Neighbors (KNN) is a simple algorithm in which its principle is to find a predefined number of training samples closest in distance to the new point, and predict the label from these. Being a non-parametric method, it is often successful in classification situations where the decision boundary is very irregular [8].
- Decision Trees (DT) algorithm consists of split nodes and leaf nodes. Each split node performs a split decision and routes a data sample either to the left or the right child node. In the tree structures, leaves represent the labels, non-leaf nodes are the input features, and branches represent conjunctions of features that lead to the classifications [9, 10].

- Support Vector Machine (SVM) algorithm is a powerful and versatile machine learning model, particularly well suited for classification of complex small- or medium-sized datasets. In this algorithm, the data is plotted in a  $n$ -dimensional space (number of features) and a decision boundary (hyperplane) split it into classes [7, 6].
- Convolutional Neural Networks (CNNs) emerged from the study of the brain's visual cortex. The most important building block is the convolutional layer. The CNN's architecture consists of several connected layers allowing the network to concentrate on small low-level features in the first hidden layer, then assemble them into larger higher-level features in the next layer, and so on [7].

#### b) *Unsupervised learning*

In unsupervised learning the training data is unlabeled. One of the most important unsupervised learning algorithms is  $k$ -means.  $K$ -means is a simple algorithm capable of clustering an unlabeled dataset very quickly and efficiently, often in just a few iterations. Its goal is to group similar instances together into clusters. The number of  $k$  clusters that the algorithm must find is specified to easily assign each instance to one of the  $k$  clusters [7].

#### 3) *Dominant colors*

The dominant colors refer to the principal colors presented in an image. The dominant colors of an image are selected grouping the image pixels according to their color in the selected color space (RGB and CIELab). The average color of each group are the dominant colors and the number of pixels of that groups are the percentage of the dominant colors.

In RGB (Red, Green, Blue), the light spectra of varying fractions of the three primary colors referred to as channels, combine to make new colors. Each channel has intensity values from 0 to 1 that are scaled by the number of bits used to represent each component. The 24-bit color cube used in this research has components in the range of 0–255. Each color in the color space can be represented as a three-value vector [11].

On the other hand, CIELab has the property of being perceptually uniform (useful to measure the similarity between two given colors) and is designed to approximate human vision. The L channel which represents the brightness of each pixel varies between 0 and 100. The a (red/green) and b (yellow/blue) channels which correspond to the chromaticity components contain information about the color of a pixel, independent of its brightness. Their values vary between -127 and 127 [12, 13].

#### 4) *Underlying technologies*

##### a) *Scikit learn*

Scikit-learn is a Python module that integrates a wide range of state-of-the-art machine learning algorithms for medium-scale supervised and unsupervised problems. This package focuses on bringing machine learning to non-specialists using a general-purpose high-level language. Emphasis is put on ease of use, performance, documentation, and API consistency. It has minimal dependencies and is distributed under the simplified Berkeley Source Distribution (BSD) license, encouraging its use in both academic and commercial settings [14].

##### b) *Tensorflow*

TensorFlow<sup>1</sup> is an interface for expressing machine learning algorithms and an implementation for executing such algorithms. A computation expressed using TensorFlow can be executed with little or no change on a wide variety of heterogeneous systems, ranging from mobile devices such as phones and tablets up to large-scale distributed systems of hundreds of machines and thousands of computational devices such as GPU cards [15].

##### c) *Tensorflow Lite*

TensorFlow Lite<sup>2</sup> is a set of tools to help developers run TensorFlow models on mobile, embedded, and IoT devices. It enables on-device machine learning inference with low latency and a small binary size [16].

TensorFlow Lite consists of two main components:

- The TensorFlow Lite interpreter, which runs specially optimized models on many different hardware types, including mobile phones, embedded Linux devices, and microcontrollers.
- The TensorFlow Lite converter, which converts TensorFlow models into an efficient form for use by the interpreter, and can introduce optimizations to improve binary size and performance.

##### d) *Swift*

Swift<sup>3</sup> is an open source programming language designed for macOS, iOS, watchOS, tvOS, and more. Swift already supports all Apple platforms and Linux, with community members actively working to port to even more platforms [17]. In 2010, Apple started developing Swift, a new programming language that would rival Objective-C in type safety, security, and hardware performance. Swift is more than 2.6x faster than Objective-C and more than 8.4x faster than Python [18].

##### e) *Xcode*

Xcode<sup>4</sup> is a long-standing tool for app production and a well-known integrated development environment (IDE), enabling developers to write the code and compile apps that can be used on a variety of different devices and operating systems [19]. It also includes a unified macOS SDK and all the frameworks, compilers, debuggers, and other tools necessary to build applications that run natively on Apple devices [20].

##### f) *CocoaPods*

CocoaPods<sup>5</sup> is a dependency manager for Swift and Objective-C Cocoa projects. The dependencies of the projects just are specified in a single text file called Pod file. CocoaPods resolves dependencies between libraries, fetches the resulting source code, then links it together in an Xcode workspace to build a single project [21].

#### B. *Related Work*

Over the last decade, there has been considerable progress in the application of machine learning to geochemistry [28]. In this section we present relevant research work in three areas:

<sup>1</sup><https://www.tensorflow.org>

<sup>2</sup><https://www.tensorflow.org/lite>

<sup>3</sup><https://swift.org>

<sup>4</sup><https://developer.apple.com/xcode/>

<sup>5</sup><https://cocoapods.org>

Table I  
COMPARISON TABLE OF THE ARTICLES DESCRIBED IN THE RELATED WORK

Author	Year	Dataset	Algorithm of extraction	Extracted features	Dataset for training	Best trained model	Results
E. Vázquez and H. Alférez [ref]	2021	846 patches from 71 images of six plutonic rock types (diorite, gabbro, granite, monzodiorite, and tonalite)	-	-	50% of the patches	4-layer structure CNN	Model accuracy: 95% Android application accuracy results: 70% for gabbro, 28.5% for diorite, 100% for granodiorite, and 28.5% for granite
Fan et al. [22]	2020	3,208 images of 28 rock lithology categories	-	-	80% of the images	SqueezeNet and MobileNet	Android application accuracies: 94.55% and 93.27% File sizes: 9.2 MB and 17.6 MB Execution times: 736 to 366 and 1,218 to 523 millisecond
Fan et al. [23]	2020	3,795 images of 30 different rock types	-	-	80% of the images	ShuffleNet	Android application accuracy: 97.65% Occupation space on PC: 18.2M Classification time: 786 millisecond
Ran et al. [24]	2019	14,589 patches from 2,290 images of six rock types (granite, limestone, conglomerate, sandstone, shale, mylonite)	-	-	60% of the patches	3-layer structure CNN	Model accuracy: 97.76% -
Zhang et al. [25]	2019	481 images of four minerals (K-feldspar, perthite, plagioclase, and quartz)	Inception-v3 CNN model	High-level features (such as chromatic aberration and texture)	90% of extracted features	Stacking model (LR, SVM, and MLP)	Model accuracy: 90.9% -
Maitre et al. [26]	2019	3,192 sub-images of the view taken to a surface with 27 mineral grains species	Simple Linear Iterative Clustering (SLIC) algorithm	Color intensity and Peak intensity of computed histograms from superpixels	70% of extracted features	Random Forest (RF)	Model accuracy: 89% -
Cheng and Guo [27]	2017	4,200 images of three feldspar sandstones rock types (coarse, medium granular, and fine)	-	-	75% of the images	6-layer structure CNN	Model accuracy: 98.5% -

image classification of rock lithology using machine learning, rock classification with machine learning on Android devices, and recognition of mineral images applying machine learning and feature extraction. Table I summarizes the works presented in this section.

#### 1) Image classification of rock lithology using machine learning

In [24], Ran et al. proposed a CNN model for the classification of six rock types (granite, limestone, conglomerate, sandstone, shale, mylonite) and compared their results with four other common machine learning models. A total of 2,290 images were labeled according to the clarity of the rock and cropped into 14,589 sample patches of  $512 \times 512$  pixels compressed to  $128 \times 128$  pixels. 60% of the patches of each type of rock were selected for the training dataset, 20% for

the validation dataset, and 20% for the testing dataset. Their proposed CNN model achieved the highest overall accuracy of 97.76% compared with the other models: SVM, AlexNet, GoogleLeNet Inception v3, and VGGNet-16.

In [27], Cheng and Guo proposed a deep CNN to identify the granularity of feldspar sandstone rocks in images under three color spaces: RGB, YCbCr, and HSV. A total of 4,200 images were collected from rocks of an oil field in Ordos and divided into three types of granularity: coarse, medium granular, and fine. The RGB images were normalized to  $224 \times 224$  pixels and converted to YCbCr and HSV. The proposed CNN was a 6-layer structure of 4 convoluted layers with ReLU as the activation function and 2 fully connected layers with Softmax as the classifier. The model was trained for each color space with 75% of the experimental data, a batch size of 100, and different kernel sizes and learning rates. The lowest

error rates were obtained with the learning rate of 0.0005, the kernel sizes of 11, 5, 3, and 3 for each convolutional layer respectively, and the cross-validation for HSV color space. In RGB color space, the classification accuracy achieved 98.5%.

## 2) Rock classification with machine learning on Android devices

In [22], Fan et al. created a method for rock lithology recognition on Android devices based on the two lightweight SqueezeNet and MobileNet CNNs. These models were compared with ResNet50, a heavyweight model. The images were selected from the China Geological Survey dataset that contains images of 28 rock categories taken by a smartphone camera. The 3,208 images were reduced to  $214 \times 214$  pixels and the 80% were used to train the two CNNs pretrained with ImageNet dataset. The achieved occupation sizes were 19.6 M and 36.8 M for MobileNet and SqueezeNet, and 232.7 M for ResNet50. SqueezeNet was almost two times faster than MobileNet, and 7 times faster than ResNet50. A rock recognition software based on the trained models was developed for Android devices. The results for SqueezeNet and MobileNet on Android smartphones were as follows: the file sizes of 9.2 MB and 17.6 MB, the execution time from 736 to 366 and 1,218 to 523 milliseconds, and the recognition accuracies of 94.55% and 93.27%.

Also in [23], Fan et al. improved their work using a model based on ShuffleNet for quick and accurate rock lithology recognition with smartphones and compared it with their previous work of MobileNet and SqueezeNet. They selected 3,795 images of 30 different kinds of rocks collected from multiple locations in East China. The ShuffleNet model was trained using 80% of the dataset, 3,600 iteration steps, a learning rate of 0.008, and the parameters imported by the transfer learning method using the ImageNet dataset. ShuffleNet occupied a space of 18.2M compared with MobileNet, SqueezeNet, and ResNet50 that occupied 34.5M, 25M, and 219.4M respectively. An Android application was created using each model and run on three Android smartphones (Huawei, Samsung, and Oppo). The average recognition time of ShuffleNet for a single rock image was 786 milliseconds, the reached accuracy was 97.65% on PC and 95.30% on the smartphones.

In our previous work [ref], we proposed a CNN model trained with several combinations of plutonic rocks to deploy the best combination of rocks in an Android application. The dataset contained 71 images of diorite, gabbro, granite, granodiorite, monzodiorite, and tonalite which classification was based on petrographic analysis of Cretaceous granitoids collected from Peru. To increase the number of images, a new dataset of 846 patches from around  $450 \times 700$  to  $900 \times 1000$  pixels was generated from the first dataset. A deep neural network was created with 4-layer structure: two convolutional, and two fully connected layers. After each convolutional layer it was a max pooling layer of  $2 \times 2$  size, and a flatten and a dropout layers before the first and second fully connected layers respectively. Several combinations of the rock classes were trained with 50% of the image patches, 100 epochs and a batch size of 32. The best combination was with four classes of plutonic rocks (gabbro, diorite, granite and granodiorite)

achieving an accuracy of 95%, an average precision of 96%, an average recall of 95%, and an average F1-score of 95%. Finally, an Android application was developed using the proposed model trained with the best combination of rocks. The application evaluation results were: 70% for gabbro, 28.5% for diorite, 100% for granodiorite, and 28.5% for granite.

## 3) Recognition of mineral images applying machine learning and feature extraction

In [25], Zhang et al. worked on the intelligent identification for rock-mineral images using ensemble machine learning algorithms (model stacking). A total of 481 images of four minerals (K-feldspar, perthite, plagioclase, and quartz) were obtained with the camera on the top of a microscope. The target RGB images were cropped to cover the minerals and then processed to be  $299 \times 299$  pixels. A deep learning model based on Inception-v3 was adopted to extract high-level features (such as chromatic aberration and texture) from the images and train the algorithms of LR, SVM, KNN, Random Forest (RF), Multilayer Perceptron (MLP), and Gaussian Naive Bayes (GNB). LR, SVM, and MLP had a significant effect on extracted features, with higher accuracy (90.0%, 90.6%, and 89.8%) than the other models. The new features generated by this three models were employed for the model stacking in a new instance of LR. The stacking model showed a better performance than the single models, with an accuracy of 90.9%.

In [26], Maitre et al. created several models of supervised machine learning to recognize mineral grains in a sample surface containing grains of 27 different mineral species (plagioclase, augite, background, hypersthene, ilmenite, magnetite, titanite, hornblende, etc.). The surface was scanned with an automated Scanning Electron Microscopy (SEM) that assigned to each grain a mineral specie based on its chemical signature. Also several views of the same surface were taken with a stereo-zoom binocular microscope to construct a large mosaic RGB image. Both images were divided in 3,192 sub-images of  $600 \times 600$  pixels. To label the grains of the mosaic image, the simple linear iterative clustering (SLIC) algorithm was applied for superpixel segmentation to match each superpixel of the mosaic's sub-images with the superpixels of the SEM's scan sub-images. From the computed RGB superpixel histograms, the color intensity (quantile) and peak intensity (ratio between the number of pixels in the first and second maximum bins to total number of pixels) were extracted as features for each superpixels. KNN, RF, and Classification and Regression Trees (CART) algorithms were trained with 70% of the extracted features, and tested with the other 30% using the kappa statistics, precision, recall, and f1-score indicators. The RF algorithm gave the best results with a global accuracy of 89%.

## 4) Discussion

Machine learning has been an effective way for image classification in geochemistry and geosciences. Specifically, feature extraction was used in [26, 25] before training machine learning models to classify images of mineral samples. Although these works showed good results, the number of features extracted was too large and their accuracies were lower than the presented in this work. No works presented



the extraction of features in the classification of rocks.

Four articles [24, 27, 22, 23] introduce the comparison of different CNN model structures to analyze the performance of these models for rock lithology classification using all the image features. Also in our previous work [ref], several combinations of plutonic rocks were analyzed using all the image features to train a CNN model rather than extracted features. In [22, 23] and [ref] the created models were deployed on an Android mobile application for the classification of rocks. However, there are no works presenting the evaluation results of the deployment of machine learning on iOS devices.

Finally, the evaluation of the models in [24, 27, 22, 23] showed good results in the field. Nevertheless, all of them were trained with diverse types of rocks instead of use only the plutonic rock type. This type of classification becomes more difficult because rocks of a same type have very similar characteristics.

### III. RESULTS

#### A. Methodology

This section describes the steps followed in this research work.

##### 1) Getting the images of the plutonic rocks

The images of plutonic rocks were provided by the Department of Earth and Biological Sciences at Loma Linda University. The dataset contains image patches of four classes of plutonic rocks: granite, granodiorite, gabbro, and diorite with a total of 283 images. The images used in the following experiments are organized in subfolders according to their class and are available online<sup>6</sup>. Table II shows the number of images per class.

Table II  
NUMBER OF IMAGES PER CLASS

Class	Number of images
Granite	70
Granodiorite	70
Gabbro	65
Diorite	78
<b>Total of images</b>	<b>283</b>

##### 2) Preparing the data

In this step, the images were processed in order to obtain the color values of the image pixels in RGB and CIELab color spaces.

First, all files (“png”, “.jpg”, and “.jpeg”) in the subfolders of the main directory of images were processed in RGB format and labeled according to their container subfolder (e.g. processed images in the granite subfolder are labeled as granite). Thereafter, the RGB values of the image pixels were converted to CIELab values using the “rgb2lab” function of the color class imported from the Scikit-image module. In this way, it is possible to train the models in the two color spaces. The notebook with the source code for data preparation is available online<sup>7</sup>

<sup>6</sup><https://github.com/sarah-hs/Color-extraction/tree/main/Rock-images>

<sup>7</sup><http://bit.ly/3pyh3JL>

##### 3) Determining the best number of color clusters

The k-means algorithm was used to extract the dominant colors from the images. The Elbow method was used to calculate the optimal number of clusters to use in k-means. This method consists of iterating in a range of possible cluster numbers and determine the best one. We selected the pixel values of one processed image to train k-means. The range of 2 to 20 was declared to obtain the scores of k-means at each cluster number. Lastly, we plotted these scores with their respective  $k$  number. The number at the elbow of the plot is the best  $k$  number of clusters, which is 4 for this experiment (see Fig. 2).

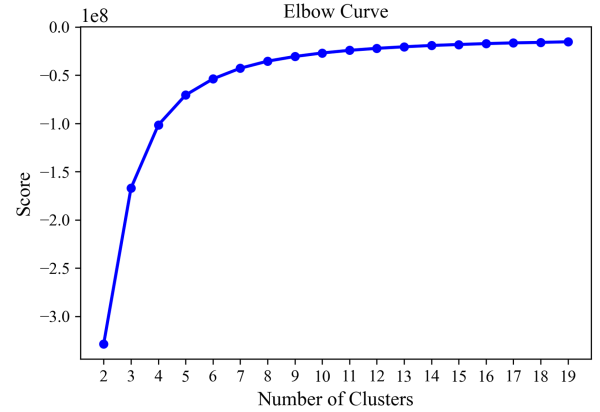


Figure 2. The Elbow method showing the optimal  $k$  number of clusters

##### 4) Color extraction

In this step the dominant colors are extracted from the rock images. In Listing 1, the “get\_dominant\_colors” function receives the pixel values of an image to train the k-means algorithm with  $k$  clusters. In line 6, k-means works by separating the pixels of the image into 4 clusters of similarly colored pixels. The colors at each cluster center reflect the average value of the attributes of all members of a cluster. The percentage of a cluster is the number of pixels within that color cluster and is calculated in lines 8 to 10. Finally, the center color of each cluster and its percentage are sorted in increasing order of percentage and added to a features list in lines 12 to 17. The returned list in line 19 are the sixteen features: the four dominant colors represented by the three channels of the selected color format and the percentage of each dominant color (see Fig. 3).

```

1 from sklearn.cluster import KMeans
2 CLUSTERS = 4
3
4 def get_dominant_colors(img):
5     reshape = img.reshape((img.shape[0] * img.shape[1],
6                             img.shape[2]))
7     cluster = KMeans(n_clusters=CLUSTERS).fit(reshape)
8
9     labels = np.arange(0,
10                        len(np.unique(cluster.labels_)) + 1)
11     (hist, _) = np.histogram(cluster.labels_, bins =
12                             labels)
13     hist = hist.astype("float"); hist /= hist.sum()
14
15     features = []
16
17     colors = sorted([(percent, color) for (percent,
18                                         color) in zip(hist, cluster.cluster_centers_)])

```

```

15 for (percent, color) in colors:
16     features.extend(color)
17     features.append(percent)
18
19
20 return features

```

Listing 1. Function to extract the dominant colors from a single image

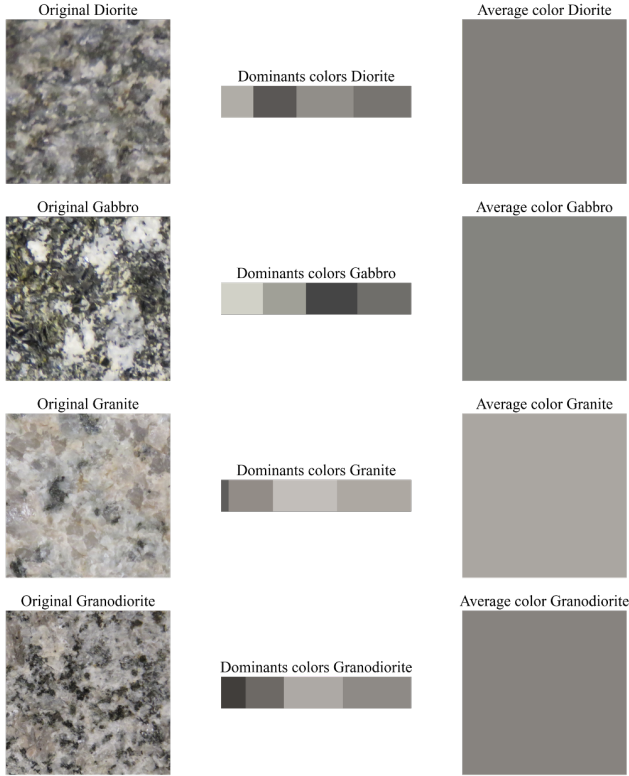


Figure 3. Dominant colors and average color of sample images

In Listing 2, the processed data in RGB format is iterated in lines 4 to 6 and to extract the dominant colors in line 5 with the function of Listing 1. The colors are added to a new list of extracted colors in line 6. This process is also made for the CIELab data in lines 8 to 10. Finally, the extracted colors in RGB and CIELab formats are saved together with their respective rock label in different CSV files. This files were used in the next step to train the machine learning algorithms. The CSVs are available online<sup>89</sup>.

```

1 extracted_colors = []
2 for img in images:
3     features = get_dominant_colors(img)
4     extracted_colors.append(features)
5
6 data_df = pd.DataFrame(extracted_colors, files)
7 data_df[16] = y
8 data_df.to_csv(CSV_DIR, header=None)

```

Listing 2. Iterate original data to extract dominant colors

##### 5) Data normalization and label encoding

First, in this step we loaded the extracted colors data from the CSVs. The dominant colors and their percentage are the

data features loaded into  $x$ , and the rock classes are the data labels loaded into  $y$ . Second, in order to train and test the models, the  $x$  and  $y$  data was divided into a train set of 80% and a test set of 20% using the “train\_test\_split” function of the model\_selection class from Scikit-learn. Third, we normalized the  $x$  data using the “MinMaxScaler” function imported from the preprocessing class of Scikit-learn. This function scales each feature to a given range of 0 to 1 for data cleaning and better performance in model training. Finally, we encoded the  $y$  data in order to transform the labels into values from 0 to 3 representing the four rock classes of diorite, gabbro, granite, and granodiorite respectively. The encoding process was made with the “LabelEncoder” function of the preprocessing class imported from Scikit-learn module.

##### 6) Training the different algorithms with the extracted dominant colors

Five machine learning models were trained using the RGB data and after the CIELab data in this experiment: LR, KNN, DT, SVM, and a CNN. The notebook showing the code for training and validation of the generated models is available online<sup>10</sup>.

Listings 3-7 present the set and training process of the models. The LR, KNN and CNN models were trained with the normalized data while the DT and SVM models with non-normalized data. The following configurations were used to set the models:

LR was created in line 3 of Listing 3 with the L-BFGS (Limited-memory Broyden–Fletcher–Goldfarb–Shanno) solver which is one of the quasi-Newton methods that approximate the BFGS algorithm, which utilizes a limited amount of computer memory. The solver’s methodology starts iterating at a random point ( $x_t$ ) to calculate the minimum from the second derivate of the original function at that point and assign it to a new point ( $x_{t+1}$ ). The new point will become the starting point for the next iteration. In this way, L-BFGS quickly converges on the solution [29].

```

1 # Logistic Regression
2 from sklearn.linear_model import LogisticRegression
3 logReg = LogisticRegression(solver='lbfgs')
4 logReg.fit(xtrainNorm, ytrain)

```

Listing 3. Configuration and training of LR

The number of neighbors used for KNN in line 3 of Listing 4 represents the neighbor samples analyzed from the dataset to classify a new sample into the class to which most of their neighbors belong.

```

1 # K-Nearest Neighbors
2 from sklearn.neighbors import KNeighborsClassifier
3 knn = KNeighborsClassifier(n_neighbors=1)
4 knn.fit(xtrainNorm, ytrain)

```

Listing 4. Configuration and training of KNN

By using class weights, we can increase the importance of a particular class during training. DT is created set in line 3 of Listing 5 with the balanced mode for class weight that uses the label values of the training set to automatically adjust the

<sup>8</sup>[https://github.com/sarah-hs/Color-extraction/blob/main/colors\\_RGB.csv](https://github.com/sarah-hs/Color-extraction/blob/main/colors_RGB.csv)

<sup>9</sup>[https://github.com/sarah-hs/Color-extraction/blob/main/colors\\_LAB.csv](https://github.com/sarah-hs/Color-extraction/blob/main/colors_LAB.csv)

<sup>10</sup><https://github.com/sarah-hs/Color-extraction/blob/main/ML-training.ipynb>

node weights inversely proportional to the class frequencies in the input data [29].

```
1 # Decision Trees
2 from sklearn.tree import DecisionTreeClassifier
3 decisionTree =
4   DecisionTreeClassifier(class_weight='balanced')
5 decisionTree.fit(xtrain, ytrain)
```

Listing 5. Configuration and training of DT

SVM is created in line 3 of Listing 6 with the Radial Basis Function (RBF) kernel which is useful to eliminate the computational requirement of the algorithm. When training an SVM with RBF, the parameter gamma must be considered. The auto value of gamma in Scikit-learn is represented by  $1/\text{numberOfFeatures}$ . Gamma defines how much influence a single training example has. The larger gamma is, the closer other examples must be to be affected [30].

```
1 # Support Vector Machines
2 from sklearn.svm import SVC
3 svmc = SVC(kernel='rbf', gamma='auto')
4 svmc.fit(xtrain, ytrain)
```

Listing 6. Configuration and training of SVM

The proposed CNN model is a four-layer structure: two one dimensional convolutional layers and two fully connected layers. There is a maxpooling layer after each convolutional layer and a flatten layer is placed between the two convolutional layers and the fully connected layers. Table III describes the structure of the CNN model created in Listing 7.

Table III  
CNN MODEL STRUCTURE

Layer	Filters	Kernel size	Activation function	Output shape
Input features	-	-	-	16
Conv1D	32	2	RELU	16 × 32
MaxPooling1D	-	2	-	8 × 32
Conv1D	64	2	RELU	8 × 64
MaxPooling1D	-	2	-	4 × 64
Flatten	-	-	-	256
Dense	64	-	RELU	64
Dense	4	-	Softmax	4

In line 7 of Listing 7 the sequential model of the Keras<sup>11</sup> library from Tensorflow was created. This model is formed by layers where each layer has exactly one input tensor and one output tensor. In lines 8 and 10 two convolutional layers of one dimension were added to the model using RELU as their activation function, 2 as kernel size, and a total of 32 and 64 filters respectively. This kind of layer creates a convolution kernel that is convolved with the layer input to produce a tensor of the output filters dimension. Moreover, RELU applies the Rectified Linear Unit activation function which is used to achieve non-linearity converting the negative values of the output tensor to 0 value after convolution operation [31]. In lines 9 and 11 the maxpooling layers are

added with a size of 2 after each convolutional layer. This kind of layer downsamples the input by taking the maximum value over a window defined by pool size. In line 12 the flatten layer flattens the input to one dimension. In lines 13 and 14 two fully connected layers are added using 64 and 4 as their number of filters, the activation functions of RELU and Softmax respectively. The Softmax function is generally used in the output layer because it normalizes a vector containing  $K$  elements into a probability distribution over the  $K$  elements. In this case, the last layer 4 filters are the CNN output tensor that contains the probabilities of the four rock classes [32]. In line 15, the model was compiled with the categorical crossentropy loss function and the Adam optimizer. Categorical cross-entropy is the most diffused classification cost function, adopted by logistic regression and the majority of neural architectures. This convex function can be easily optimized using stochastic gradient descent techniques and is an excellent choice for classification problems [33]. On the other hand, Adam (adaptive moment estimation) algorithm is an efficient optimization method that computes adaptive learning rates for each parameter to optimize the weights of the model [29]. Finally, to train the CNN several numbers of epochs and batches were tried until the most optimal values were obtained as shown in line 19.

```
1 # Convolutional Neural Network
2 from tensorflow.keras.models import Sequential
3 from tensorflow.keras.layers import Dense, Flatten,
4   Dropout, Conv1D, MaxPooling1D
5 from tensorflow.keras import optimizers
6 from livelossplot.inputs.tf_keras import
7   PlotLossesCallback
8
9 model = Sequential()
10 model.add(Conv1D(32, kernel_size=2, padding="same",
11   input_shape = (16, 1), activation='relu'))
12 model.add(MaxPooling1D(pool_size=2))
13 model.add(Conv1D(64, kernel_size=2, padding="same",
14   activation='relu'))
15 model.add(MaxPooling1D(pool_size=2))
16 model.add(Flatten())
17 model.add(Dense(64, activation='relu'))
18 model.add(Dense(len(classes_dict),
19   activation='softmax'))
20 model.compile(loss='sparse_categorical_crossentropy',
21   optimizer='adam', metrics=['accuracy'])
22
23 xtrain2 = np.expand_dims(xtrainNorm, 2)
24 ytrain2 = np.expand_dims(ytrain, 1)
25 model.fit(xtrain2, ytrain2, epochs=100, batch_size=32)
```

Listing 7. Configuration and training of CNN

## 7) Evaluation of the machine learning algorithms

Evaluating a supervised learning algorithm during the evaluation and testing phases is an essential part of any well-made machine learning pipeline. The following four metrics were used in this project to evaluate the algorithms:

- Accuracy is the ratio of the number of correct predictions made to the number of all predictions made [34].

$$\text{Accuracy} = \frac{\text{CorrectPredictions}}{\text{PredictionsMade}}$$

- Precision is the number of correct positives results, divided by the number of positive results predicted [34].

$$\text{Precision} = \frac{TP}{TP + FP}$$

<sup>11</sup><https://keras.io>

- Recall is the number of correct positive results, divided by the number of all relevant samples (all the samples that should be classified as positive) [34].

$$Recall = \frac{TP}{TP + FN}$$

- F1-score is the harmonic mean between precision and recall. This number, which is in the [0,1] range, indicates how precise the classifier is (precision) and how robust it is (recall). The greater the F1 score, the better the overall performance of the model [34].

$$F1 = 2 * \frac{Precision * Recall}{Precision + Recall}$$

Table IV shows the accuracy results of the algorithms evaluated with the test set of dominant colors in RGB and CIELab color formats.

Table IV  
RESULTS OF ALL THE ALGORITHMS IN TERMS OF ACCURACY

Model	Accuracy	
	RGB	CIELab
Logistic Regression	0.63	0.63
KNN	0.79	0.93
Decision Trees	0.73	0.72
SVM	0.52	0.80
CNN	0.68	0.82

Tables V-IX show the results of each model evaluation in terms of precision, recall and F1-score for each RGB and CIELab color spaces. The best results were obtained with the KNN model using the CIELab color space with the highest average values of accuracy, precision, recall, and F-score equal to 93%.

Table V  
RESULTS OF LOGISTIC REGRESSION

Class	Precision		Recall		F1-score	
	RGB	LAB	RGB	LAB	RGB	LAB
Granite	0.72	0.81	1.00	1.00	0.84	0.90
Granodiorite	0.62	0.64	0.36	0.50	0.45	0.56
Gabbro	0.53	0.50	0.77	0.77	0.62	0.61
Diorite	0.67	0.60	0.47	0.35	0.55	0.44
Average	<b>0.64</b>	<b>0.64</b>	<b>0.65</b>	<b>0.66</b>	<b>0.62</b>	<b>0.63</b>

Table VI  
RESULTS OF K-NEAREST NEIGHBORS

Class	Precision		Recall		F1-score	
	RGB	LAB	RGB	LAB	RGB	LAB
Granite	0.85	1.00	0.85	0.92	0.85	0.96
Granodiorite	0.92	0.92	0.79	0.79	0.85	0.85
Gabbro	0.71	0.93	0.77	1.00	0.74	0.96
Diorite	0.72	0.89	0.76	1.00	0.74	0.94
Average	<b>0.80</b>	<b>0.93</b>	<b>0.79</b>	<b>0.93</b>	<b>0.79</b>	<b>0.93</b>

Table VII  
RESULTS OF DECISION TREES

Class	Precision		Recall		F1-score	
	RGB	LAB	RGB	LAB	RGB	LAB
Granite	0.92	0.86	0.85	0.92	0.88	0.89
Granodiorite	0.62	0.73	0.71	0.57	0.67	0.64
Gabbro	0.67	0.56	0.77	0.69	0.71	0.62
Diorite	0.79	0.75	0.65	0.71	0.71	0.73
Average	<b>0.75</b>	<b>0.72</b>	<b>0.74</b>	<b>0.72</b>	<b>0.74</b>	<b>0.72</b>

Table VIII  
RESULTS OF SUPPORT VECTOR MACHINE

Class	Precision		Recall		F1-score	
	RGB	LAB	RGB	LAB	RGB	LAB
Granite	1.00	0.87	0.69	1.00	0.82	0.93
Granodiorite	1.00	0.80	0.29	0.57	0.44	0.67
Gabbro	0.00	0.68	0.00	1.00	0.00	0.81
Diorite	0.39	0.92	1.00	0.71	0.56	0.80
Average	<b>0.60</b>	<b>0.82</b>	<b>0.49</b>	<b>0.82</b>	<b>0.46</b>	<b>0.80</b>

Table IX  
RESULTS OF THE CONVOLUTIONAL NEURAL NETWORK

Class	Precision		Recall		F1-score	
	RGB	LAB	RGB	LAB	RGB	LAB
Granite	0.81	0.93	1.00	1.00	0.90	0.96
Granodiorite	0.70	0.67	0.50	0.57	0.58	0.62
Gabbro	0.61	0.81	0.85	1.00	0.71	0.90
Diorite	0.62	0.87	0.47	0.76	0.53	0.81
Average	<b>0.68</b>	<b>0.82</b>	<b>0.70</b>	<b>0.83</b>	<b>0.68</b>	<b>0.82</b>

## B. Results

The KNN model was the model deployed in the iOS mobile application to make the classification of images of four classes of plutonic rocks in real time. The Xcode IDE, the Xcode command-line tools, a valid Apple Developer ID, and the CocoaPods dependency manager were the main requirements to develop the application. The application is written mostly in Swift and uses the following two libraries for performing the dominant colors extraction and image classification:

- The DominantColor<sup>12</sup> dependency is an open source library written in Swift and created by Indragie Karunaratne. It finds the dominant colors of an image using the CIELab color space and the k-means clustering algorithm. In this project an adaptation of this library was implemented exporting code from the 7 main files of the repository into the application project.
- The TensorFlowLite Swift<sup>13</sup> library is TensorFlow's lightweight solution for Swift developers. It enables low-latency inference of on-device machine learning models with a small binary size and fast performance supporting hardware acceleration. For the application, TensorFlowLiteSwift pod name was added into the project's Podfile, and from command line the library was resolved into the Xcode project by the CocoaPods dependency manager.

<sup>12</sup><https://github.com/indragiek/DominantColor>

<sup>13</sup><https://github.com/tensorflow/tensorflow/tree/master/tensorflow/lite/swift>

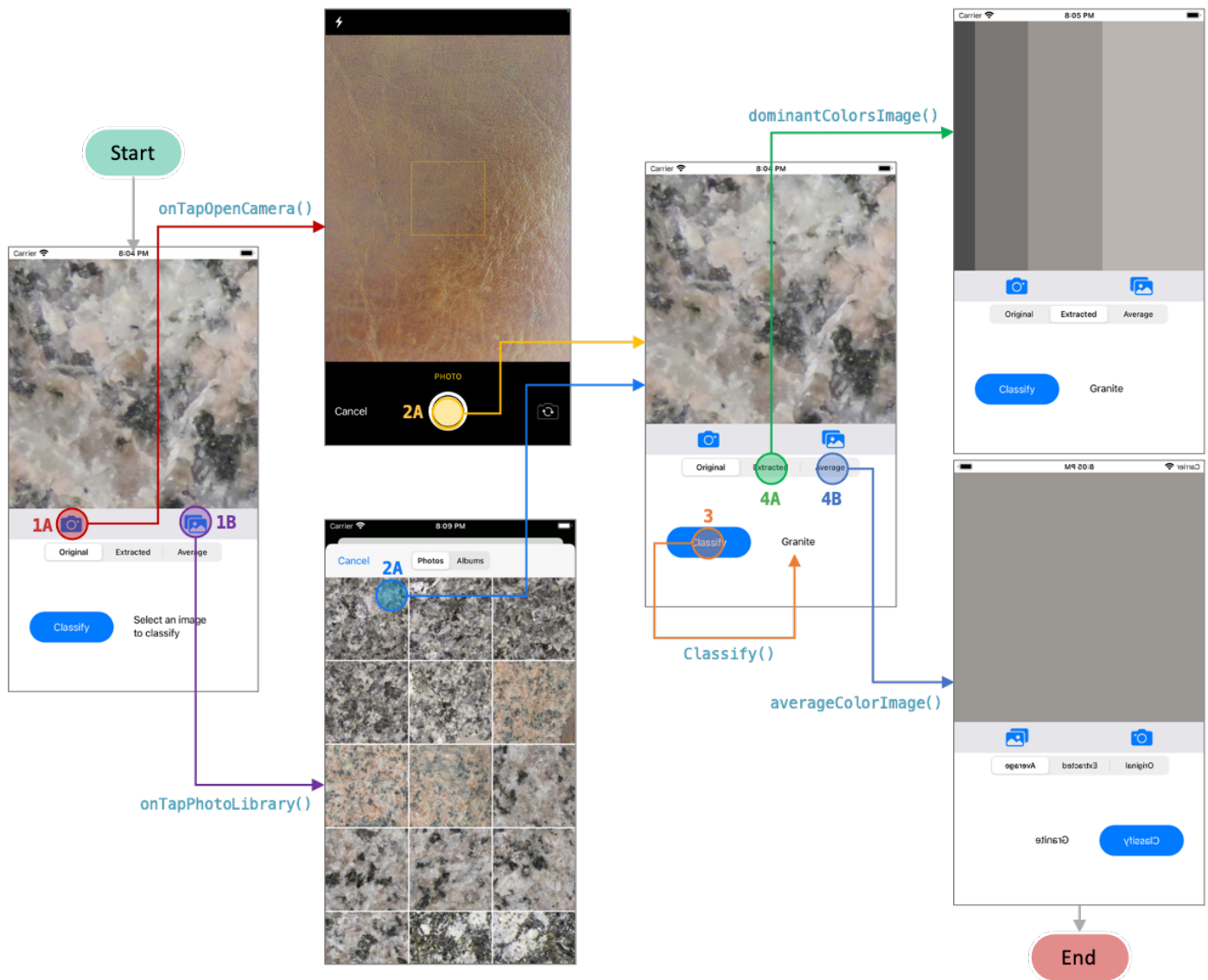


Figure 4. Application workflow

As a required step for the deployment of the KNN model in the application it was necessary to export the model by creating and training a concrete function in TensorFlow. This function calculates the Manhattan distance of a new data point to all the points in training data to select the label of the nearest point as the label of the new point. The last step in the model exportation was to create a graph of the trained model from the concrete function. That graph was exported in a file with tflite extension using TensorFlow Lite. The source code of the creation and exportation of KNN in TensorFlow is available online<sup>14</sup>.

Listed below is the application process (see Fig. 4). The source code of the application is available online<sup>15</sup>.

There are two ways to make the classification on the iOS application. The first way is to take a picture with the OpenCamera button that is showed in step 1A of Fig. 4.

When camera opens, a new scene appears displaying the device camera to take the picture as shown in step 2A. The second way is choosing a photo from the Photo Library. The OpenLibrary button of step 1B opens the photo library screen of the iOS device as is shown in step 2B.

After the image was loaded the extraction is performed with the `dominantColorsInImage` function imported from the `DominantColor` library. Thereafter, the `Classify` button in step 3 is enabled to classify the new rock image into: granite, granodiorite, gabbro, and diorite. At this step the previous extracted colors are converted to a buffer of CIELab color data. This colors are sorted in descendet order by their percentage of pixels in the image and used as the input tensor for the tflite file containing the graph of the KNN model. Optionally, the dominant colors and the average colors of the selected image can be displayed pressing the `Extracted` and `Average` buttons of steps 4A and 4B respectively as shown in Fig. 4.

<sup>14</sup><https://github.com/sarah-hs/Color-extraction/blob/main/ML-training.ipynb>

<sup>15</sup><https://github.com/sarah-hs/Rock-Classifer-iOS>



### C. Discussion

Five machine learning algorithms were trained with just the four dominant colors extracted from images of plutonic rocks. The best algorithm in this experiment was K-Nearest Neighbors trained with the dominant colors in the CIELAB color format of 283 images. Its values of accuracy, precision, recall, and F-score average were equal to 93%. Table X presents the comparison of these results and the results of our previous approach with a CNN using all the image features [ref].

Table X  
COMPARISON OF THE BEST MODELS IN THIS RESEARCH AND THE BEST MODEL PRESENTED IN OUR PREVIOUS WORK

Metrics	KNN of this work with four dominant colors	CNN of our previous work [ref] with all the features used during training
Accuracy	93%	95%
Precision	93%	96%
Recall	93%	95%
F1-score	93%	95%

The application running the K-Nearest Neighbors model was tested in the field with 34 images and the following average accuracy results were obtained: 85.7% for granite, 20% for granodiorite, 70% for gabbro, and 28.5% for diorite. Table XI shows its comparison with the results of the Android application of our previous work in the field.

Table XI  
RESULTS COMPARISON OF THE IOS APPLICATION AND THE ANDROID APPLICATION OF OUR PREVIOUS WORK IN THE FIELD

Class	Taken images	Correctly classified in this work		Correctly classified in our previous work	
		Images	Percent	Images	Percent
Granite	7	6	85.7%	2	28.5%
Granodiorite	10	2	20%	10	100%
Gabbro	10	7	70%	7	70%
Diorite	7	2	28.5%	2	28.5%
<b>Total</b>	<b>34</b>	<b>17</b>	<b>50%</b>	<b>21</b>	<b>61%</b>

The high accuracy value when classifying granite samples was because, in general, their dominant colors tend to be noticeably lighter than in the samples of the other three classes. It is also the case for gabbro with dark dominant colors. In contrast, granodiorite share characteristics of both granite and diorite. Therefore, it is more difficult to automatically classify granodiorite based on their dominant colors. Also, diorite tended to be confused with granodiorite. According to the results in the field, our hypothesis was not fulfilled. The results for granodiorite and diorite show the need for improving the classification model with a higher number of images that cover a variety of colors per class.

## IV. CONCLUSIONS AND FUTURE WORK

### REFERENCES

[1] National Geographic Society, *Igneous rocks*, English, ENCYCLOPEDIA ENTRY, Access date: 12/16/2020,

National Geographic, Oct. 2019. [Online]. Available: <https://www.nationalgeographic.org/encyclopedia/igneous-rocks/>.

[2] R. Gillaspay, *Volcanic vs plutonic igneous rocks: Definition and differences*, English, Access date: 12/16/2020, Study.com, Nov. 2013. [Online]. Available: <https://study.com/academy/lesson/volcanic-vs-plutonic-igneous-rocks-definition-and-differences.html>.

[3] Natural Resources Conservation Service, "Part 631: Geology," in *National Engineering Handbook*, 210-VI, Access date: 12/16/2020, 2012, ch. 4, p. 7. [Online]. Available: <https://directives.sc.egov.usda.gov/OpenNonWebContent.aspx?content=31848.wba>.

[4] f. y. n., *RACEFEN Glosario de geología*, Spanish, Access date: 01/04/2021, España: Real academia de ciencias exactas, físicas y naturales. [Online]. Available: [http://www.ugr.es/~agcasco/personal/rac\\_geologia/0\\_rac.htm](http://www.ugr.es/~agcasco/personal/rac_geologia/0_rac.htm).

[5] Encyclopædia Britannica, *Diorite*, English, Access date: 12/15/2020, Encyclopædia Britannica, Jan. 2009. [Online]. Available: <https://www.britannica.com/science/diorite>.

[6] P. Harrington, *Machine Learning in Action*. MANNING PUBN, Apr. 1, 2012, 384 pp., ISBN: 1617290181. [Online]. Available: <https://www.manning.com/books/machine-learning-in-action>.

[7] A. Géron, *Hands-on Machine Learning with Scikit-Learn, Keras, and TensorFlow*. O'Reilly UK Ltd., Oct. 1, 2019, 819 pp., ISBN: 1492032646. [Online]. Available: <https://learning.oreilly.com/library/view/hands-on-machine-learning/9781492032632/>.

[8] Scikit-learn, *Nearest Neighbors*, English, Access date: 12/15/2020, Scikit-learn. [Online]. Available: <https://scikit-learn.org/stable/modules/neighbors.html#id5>.

[9] C. Reinders, H. Ackermann, M. Y. Yang, and B. Rosenhahn, "Chapter 4 - Learning Convolutional Neural Networks for Object Detection with Very Little Training Data," in *Multimodal Scene Understanding*, M. Y. Yang, B. Rosenhahn, and V. Murino, Eds., Academic Press, 2019, pp. 65–100, ISBN: 978-0-12-817358-9. DOI: <https://doi.org/10.1016/B978-0-12-817358-9.00010-X>. [Online]. Available: <http://www.sciencedirect.com/science/article/pii/B978012817358900010X>.

[10] L. Tan, "Chapter 17 - Code Comment Analysis for Improving Software Quality," in *The Art and Science of Analyzing Software Data*, C. Bird, T. Menzies, and T. Zimmermann, Eds., Boston: Morgan Kaufmann, 2015, pp. 493–517, ISBN: 978-0-12-411519-4. DOI: <https://doi.org/10.1016/B978-0-12-411519-4.00017-3>. [Online]. Available: <http://www.sciencedirect.com/science/article/pii/B9780124115194000173>.

[11] S. Wallace, *Perl Graphics Programming*. O'REILLY MEDIA, Dec. 1, 2002, 478 pp., ISBN: 059600219X. [Online]. Available: <https://learning.oreilly.com/library/view/perl-graphics-programming/9781449358280/>.

[12] R. L. David Millán Escrivá, *OpenCV 4 Computer Vision Application Programming Cookbook*. Packt Publishing, May 2, 2019, 494 pp., ISBN: 1789340721. [Online].

- Available: [https://www.ebook.de/de/product/36791804/david\\_millan\\_escriva\\_robert\\_laganiere\\_opencv\\_4\\_computer\\_vision\\_application\\_programming\\_cookbook.html](https://www.ebook.de/de/product/36791804/david_millan_escriva_robert_laganiere_opencv_4_computer_vision_application_programming_cookbook.html).
- [13] D. Young, *Mastering the Nikon D90*. ROCKY NOOK, Sep. 1, 2009, 337 pp., ISBN: 1933952504. [Online]. Available: [https://www.ebook.de/de/product/8515994/darrell\\_young\\_mastering\\_the\\_nikon\\_d90.html](https://www.ebook.de/de/product/8515994/darrell_young_mastering_the_nikon_d90.html).
- [14] F. Pedregosa, G. Varoquaux, A. Gramfort, V. Michel, B. Thirion, O. Grisel, M. Blondel, P. Prettenhofer, R. Weiss, V. Dubourg, J. Vanderplas, A. Passos, D. Cournapeau, M. Brucher, M. Perrot, and E. Duchesnay, "Scikit-learn: Machine Learning in Python," *Journal of Machine Learning Research*, vol. 12, no. 85, pp. 2825–2830, 2011. [Online]. Available: <http://jmlr.org/papers/v12/pedregosa11a.html>.
- [15] M. Abadi, A. Agarwal, P. Barham, E. Brevdo, Z. Chen, C. Citro, G. S. Corrado, A. Davis, J. Dean, M. Devin, S. Ghemawat, I. Goodfellow, A. Harp, G. Irving, M. Isard, Y. Jia, R. Jozefowicz, L. Kaiser, M. Kudlur, J. Levenberg, D. Mane, R. Monga, S. Moore, D. Murray, C. Olah, M. Schuster, J. Shlens, B. Steiner, I. Sutskever, K. Talwar, P. Tucker, V. Vanhoucke, V. Vasudevan, F. Viegas, O. Vinyals, P. Warden, M. Wattenberg, M. Wicke, Y. Yu, and X. Zheng, "TensorFlow: Large-Scale Machine Learning on Heterogeneous Distributed Systems," Mar. 14, 2016, arXiv: 1603.04467 [cs.LG].
- [16] TensorFlow, *TensorFlow Lite guide*, English, comp. software, Access date: 12/15/2020, TensorFlow, Mar. 2020. [Online]. Available: <https://www.tensorflow.org/lite/guide>.
- [17] Apple, *Swift. the powerful programming language that is also easy to learn*. English, Tech. Rep., Access date: 12/15/2020, Apple. [Online]. Available: <https://developer.apple.com/swift/>.
- [18] C. Bohon, *Apple's Swift programming language*, English, Access date: 12/15/2020, TechRepublic, Sep. 2020. [Online]. Available: <https://www.techrepublic.com/article/apples-swift-programming-language-the-smart-persons-guide/>.
- [19] Apple Insider, *Xcode*, English, Tech. Rep., Access date: 12/15/2020, Apple insider, Dec. 2020. [Online]. Available: <https://appleinsider.com/inside/xcode>.
- [20] Apple, *Introducing Xcode 12*, English, tech report, Access date: 12/15/2020, Apple. [Online]. Available: <https://developer.apple.com/xcode/>.
- [21] CocoaPods, *What is CocoaPods*, English, comp. software, Access date: 01/15/2021, CocoaPods. [Online]. Available: <https://guides.cocoapods.org/using/getting-started.html>.
- [22] G. Fan, F. Chen, D. Chen, and Y. Dong, "Recognizing Multiple Types of Rocks Quickly and Accurately Based on Lightweight CNNs Model," *IEEE Access*, vol. 8, pp. 55 269–55 278, 2020. DOI: 10.1109/access.2020.2982017.
- [23] G. Fan, F. Chen, D. Chen, Y. Li, and Y. Dong, "A Deep Learning Model for Quick and Accurate Rock Recognition with Smartphones," *Mobile Information Systems*, vol. 2020, pp. 1–14, 2020. DOI: 10.1155/2020/7462524.
- [24] X. Ran, L. Xue, Y. Zhang, Z. Liu, X. Sang, and J. He, "Rock Classification from Field Image Patches Analyzed Using a Deep Convolutional Neural Network," *Mathematics*, vol. 7, no. 8, p. 755, 2019. DOI: 10.3390/math7080755.
- [25] Y. Zhang, M. Li, S. Han, Q. Ren, and J. Shi, "Intelligent Identification for Rock-Mineral Microscopic Images Using Ensemble Machine Learning Algorithms," *Sensors*, vol. 19, no. 18, p. 3914, 2019. DOI: 10.3390/s19183914.
- [26] J. Maitre, K. Bouchard, and L. P. Bédard, "Mineral grains recognition using computer vision and machine learning," *Computers & Geosciences*, vol. 130, pp. 84–93, 2019. DOI: 10.1016/j.cageo.2019.05.009.
- [27] G. Cheng and W. Guo, "Rock images classification by using deep convolution neural network," *Journal of Physics: Conference Series*, vol. 887, p. 012 089, 2017. DOI: 10.1088/1742-6596/887/1/012089.
- [28] D. J. Lary, G. K. Zewdie, X. Liu, D. Wu, E. Levetin, R. J. Allee, N. Malakar, A. Walker, H. Mussa, A. Mannino, and D. Aurin, "Machine Learning Applications for Earth Observation," in *Earth Observation Open Science and Innovation*, C. Mathieu Pierre-Philippe and Aubrecht, Ed., Cham: Springer International Publishing, 2018, pp. 165–218, ISBN: 978-3-319-65633-5. DOI: 10.1007/978-3-319-65633-5\_8. [Online]. Available: [https://doi.org/10.1007/978-3-319-65633-5\\_8](https://doi.org/10.1007/978-3-319-65633-5_8).
- [29] P. Dangeti, *Statistics for Machine Learning*. Packt Publishing, Jul. 21, 2017, 442 pp., ISBN: 1788295757. [Online]. Available: <https://www.packtpub.com/product/statistics-for-machine-learning/9781788295758>.
- [30] Scikit learn, *Support Vector Classification*, English, Access date: 01/15/2021, Scikit-learn. [Online]. Available: <https://scikit-learn.org/stable/modules/generated/sklearn.svm.SVC.html?highlight=svc#sklearn.svm.SVC>.
- [31] L. Mitchell, K. Sri. Yogesh, and V. Subramanian, *Deep Learning with PyTorch 1.x - Second Edition*. Packt Publishing, Nov. 29, 2019, 304 pp., ISBN: 1838553002. [Online]. Available: [https://www.ebook.de/de/product/38373835/laura\\_mitchell\\_sri\\_yogesh\\_k\\_vishnu\\_subramanian\\_deep\\_learning\\_with\\_pytorch\\_1\\_x\\_second\\_edition.html](https://www.ebook.de/de/product/38373835/laura_mitchell_sri_yogesh_k_vishnu_subramanian_deep_learning_with_pytorch_1_x_second_edition.html).
- [32] J. Dawani, *Hands-On Mathematics for Deep Learning*. Packt Publishing, Jun. 12, 2020, 364 pp., ISBN: 1838647295. [Online]. Available: [https://www.ebook.de/de/product/39249321/jay\\_dawani\\_hands\\_on\\_mathematics\\_for\\_deep\\_learning.html](https://www.ebook.de/de/product/39249321/jay_dawani_hands_on_mathematics_for_deep_learning.html).
- [33] G. Bonaccorso, A. Fandango, and R. Shanmugamani, *Python*. Packt Publishing, Dec. 19, 2018, 764 pp., ISBN: 1789957214. [Online]. Available: <https://www.packtpub.com/product/python-advanced-guide-to-artificial-intelligence/9781789957211>.
- [34] P. Galeone, *Hands-On Neural Networks with TensorFlow 2.0*. Packt Publishing, Sep. 13, 2019, 358 pp., ISBN: 1789615550. [Online]. Available: <https://www>.

[ebook.de/de/product/37897428/paolo\\_galeone\\_hands\\_on\\_neural\\_networks\\_with\\_tensorflow\\_2\\_0.html](https://ebook.de/de/product/37897428/paolo_galeone_hands_on_neural_networks_with_tensorflow_2_0.html).